AFRL-ML-WP-TP-2007-525

COMBINED NONLINEAR EFFECTS IN TWO-PHOTON ABSORPTION CHROMOPHORES AT HIGH INTENSITIES (PREPRINT)

Richard L. Sutherland, Daniel G. McLean, Mark C. Brant, Joy E. Rogers, Paul A. Fleitz, and Augustine M. Urbas

Hardened Materials Branch
Survivability and Sensor Materials Division

AUGUST 2006

AIR FORCE RESEARCH LABORATORY
MATERIALS AND MANUFACTURING DIRECTORATE
WRIGHT-PATTERSON AIR FORCE BASE, OH 45433-7750
AIR FORCE MATERIEL COMMAND
UNITED STATES AIR FORCE

NOTICE AND SIGNATURE PAGE

Using Government drawings, specifications, or other data included in this document for any purpose other than Government procurement does not in any way obligate the U.S. Government. The fact that the Government formulated or supplied the drawings, specifications, or other data does not license the holder or any other person or corporation; or convey any rights or permission to manufacture, use, or sell any patented invention that may relate to them.

This report was cleared for public release by the Air Force Research Laboratory Wright Site (AFRL/WS) Public Affairs Office and is available to the general public, including foreign nationals. Copies may be obtained from the Defense Technical Information Center (DTIC) (http://www.dtic.mil).

AFRL-ML-WP-TP-2007-525 HAS BEEN REVIEWED AND IS APPROVED FOR PUBLICATION IN ACCORDANCE WITH ASSIGNED DISTRIBUTION STATEMENT.

*//Signature//

PAUL A. FLEITZ, Ph.D.
Program Manager
Exploratory Development
Hardened Materials Branch

//Signature//

MARK S. FORTE, Acting Chief
Hardened Materials Branch
Survivability and Sensor Materials Division

//Signature//

TIM J. SCHUMACHER, Chief
Survivability and Sensor Materials Division

This report is published in the interest of scientific and technical information exchange, and its publication does not constitute the Government's approval or disapproval of its ideas or findings.

*Disseminated copies will show "//Signature//" stamped or typed above the signature blocks.

REPORT DOCUMENTATION PAGE

Form Approved
OMB No. 0704-0188

1. REPORT DATE *(DD-MM-YY)*	2. REPORT TYPE	3. DATES COVERED *(From - To)*
August 2006	Conference Paper Preprint	

4. TITLE AND SUBTITLE

COMBINED NONLINEAR EFFECTS IN TWO-PHOTON ABSORPTION CHROMOPHORES AT HIGH INTENSITIES (PREPRINT)

5a. CONTRACT NUMBER
In-house

5b. GRANT NUMBER

5c. PROGRAM ELEMENT NUMBER
62102F

6. AUTHOR(S)

Richard L. Sutherland, Daniel G. McLean, and Mark C. Brant (Science Applications International Corporation)
Joy E. Rogers (UES, Inc.)
Paul A. Fleitz and Augustine M. Urbas (AFRL/MLPJ)

5d. PROJECT NUMBER
4348

5e. TASK NUMBER
RG

5f. WORK UNIT NUMBER
M08R1000

7. PERFORMING ORGANIZATION NAME(S) AND ADDRESS(ES)

Science Applications International Corporation
Dayton, OH 45433

UES, Inc.
4401 Dayton-Xenia Road
Dayton, OH 45432

Hardened Materials Branch (AFRL/MLPJ)
Survivability and Sensor Materials Division
Materials and Manufacturing Directorate
Wright-Patterson Air Force Base, OH 45433-7750
Air Force Materiel Command, United States Air Force

8. PERFORMING ORGANIZATION REPORT NUMBER
AFRL-ML-WP-TP-2007-525

9. SPONSORING/MONITORING AGENCY NAME(S) AND ADDRESS(ES)

Air Force Research Laboratory
Materials and Manufacturing Directorate
Wright-Patterson Air Force Base, OH 45433-7750
Air Force Materiel Command, United States Air Force

10. SPONSORING/MONITORING AGENCY ACRONYM(S)
AFRL/MLPJ

11. SPONSORING/MONITORING AGENCY REPORT NUMBER(S)
AFRL-ML-WP-TP-2007-525

12. DISTRIBUTION/AVAILABILITY STATEMENT
Approved for public release; distribution unlimited.

13. SUPPLEMENTARY NOTES
Conference paper submitted to the Proceedings of the SPIE Optics and Photonics Conference. The U.S. Government is joint author of this work and has the right to use, modify, reproduce, release, perform, display, or disclose the work. PAO Case Number: AFRL/WS 06-1698, 10 Jul 2006.

14. ABSTRACT

Large two-photon and excited state absorption have been reported in donor-acceptor-substituted pi-conjugated molecules. We have performed detailed nonlinear absorption and photophysical measurements on a system of AFX chromophores and calculate the nonlinear transmission based on an effective three-level model. A numerical model that includes far wing linear absorption has been developed and compared with an analytical three-photon absorption model. The models are in accordance and yield excellent agreement with experimental nonlinear transmission date of 0.02-M AFX solutions up to laser intensities ~ 1GW/cm2. Concentration effects at this intensity become increasingly evident. We have extended our modeling efforts to include some new effects that may be anticipated in this regime, such as stimulated scattering are included. We report on our experimental observations of various materials and discuss results with respect to our textended theoretical models.

15. SUBJECT TERMS

16. SECURITY CLASSIFICATION OF:			17. LIMITATION OF ABSTRACT:	18. NUMBER OF PAGES	19a. NAME OF RESPONSIBLE PERSON (Monitor)
a. REPORT	b. ABSTRACT	c. THIS PAGE			Paul A. Fleitz
Unclassified	Unclassified	Unclassified	SAR	20	19b. TELEPHONE NUMBER *(Include Area Code)* N/A

Standard Form 298 (Rev. 8-98)
Prescribed by ANSI Std. Z39-18

Combined nonlinear effects in two-photon absorption chromophores at high intensities

R. L. Sutherland*[a], D. G. McLean[a], M. C. Brant[a], J. E. Rogers[b], P. A. Fleitz[c], and A. M. Urbas[c]
[a]Science Applications International Corporation, Dayton, OH, USA 45431
[b]UES, Inc., Dayton, OH, USA 45432
[c]Air Force Research Laboratory Wright-Patterson Air Force Base, OH, USA 45433

ABSTRACT

Large two-photon and excited state absorption have been reported in donor-acceptor-substituted pi-conjugated molecules. We have performed detailed nonlinear absorption and photophysical measurements on a system of AFX chromophores and calculate the nonlinear transmission based on an effective three-level model. A numerical model that includes far wing linear absorption has been developed and compared with an analytical three-photon absorption model. The models are in accordance and yield excellent agreement with experimental nonlinear transmission data for 0.02-M AFX solutions up to laser intensities ~ 1 GW/cm^2. Concentration effects at this intensity become increasingly evident. We have extended our modeling efforts to include some new effects that may be anticipated in this regime, such as stimulated scattering, molecular interactions, and saturation. Effects of chirped pulses and linewidth of the pump laser on stimulated scattering are included. We report on our experimental observations of various materials and discuss results with respect to our extended theoretical models.

Keywords: two-photon absorption, excited state absorption, nonlinear transmission, nonlinear scattering

1. INTRODUCTION

Symmetric and asymmetric electron-donor/acceptor-substituted, π-conjugated systems are a major class of enhanced two-photon absorption (TPA) materials.[1,2] The molecular TPA cross section, σ_2, is often characterized by nonlinear transmittance (NLT) experiments, both in the nanosecond and femtosecond regimes. However, the nanosecond measurements in these materials typically yield values of σ_2 larger by more than two orders of magnitude.[3,4] Excited state absorption (ESA) has been postulated to play a role in the nanosecond measurements, and for this reason the nonlinear parameters have been called effective TPA cross sections.[5,6]

TPA followed by ESA was observed as early as 1974, and a value for the product of the ESA cross section and excited state lifetime of the chromophore was estimated based on a rate equation analysis.[7] Several authors have posited the effects of excited states on nonlinear absorption and refraction, and these effects have been convincingly demonstrated in degenerate four-wave mixing and Z-scan experiments.[8-11] Evidence of ESA has been demonstrated in NLT and Z-scan measurements of organic materials[12,13], and effective (intensity dependent) TPA coefficients have been employed to estimate ESA cross sections.[3,11,14] However, to our knowledge no one has independently identified and characterized these excited states, then used this information to theoretically predict or model nanosecond NLT measurements. The nature of these excited states is important. For example, properties of the excited singlet state are significant for fluorescence imaging and laser applications, whereas the triplet state plays an important role in photopolymerization and photodynamic therapy. Moreover, the intrinsic (pulse-width independent) value of the TPA cross section σ_2 as well as the significance of ESA in comparison to other potential nonlinear mechanisms, such as stimulated scattering, self-focusing/defocusing, and possibly two-step TPA[15], need to be elucidated for accurate modeling of nonlinear absorption in the nanosecond regime.[13] Our goal is to ensure that all of the material parameters necessary to model the NLT are independently characterized. Eliminating these other phenomena as potential sources of NLT simplifies the modeling.

Recently, He et al. reported the observation of stimulated backscattering in a two-photon absorption medium, where the frequency of the stimulated wave was identical to the incident laser frequency (within the resolution of their interferometer), and the small-signal gain was quadratic in the incident laser intensity.[16,17] They considered a stimulated thermal

*sutherlandr@saic.com

Rayleigh scattering model based on TPA-enhanced temperature and density fluctuations, but ruled this out due to (a) the broad linewidth of their pump laser, which would severely reduce the gain of the stimulated wave, and (b) the fact that the peak gain in this theory is for an anti-Stokes-shifted wave, contrary to their experimental results. They concluded that the stimulated wave was due to a Bragg grating formed by the superposition of the incident laser beam and an elastically (Rayleigh) backscattered wave, creating an index grating via a TPA-resonance enhanced nonlinear index coefficient n_2, i.e., a Kerr effect. The stimulated backscattered wave is then due to reflection of the laser from this grating.

Two-beam coupling (TBC) has a rich history in nonlinear optics. Early studies established two conditions for one-way energy transfer between two electromagnetic waves in a Kerr medium: 1) the frequencies must be nondegenerate, and 2) the nonlinearity of the medium must have a finite response time.[18] The nonlinear refractive index is usually assumed to obey a simple Debye relaxation model. Energy transfer under these conditions is always from the high frequency beam to the low frequency beam for a positive Kerr nonlinearity. Silberberg and Joseph showed that counter-propagating beams in such a Kerr medium can exhibit optical instabilities and self-oscillation,[18,19] while Yeh gave an exact solution for energy transfer between two co-propagating beams including the effect of linear absorption.[20] In each of these studies, both beams had non-zero input values.

TBC also describes several stimulated scattering phenomena, such as stimulated Raman (SRS), Brillouin (SBS), and Rayleigh-wing scattering (SRWS). The Stokes (down-shifted frequency) wave in these phenomena arises internally from scattered light and experiences gain at the expense of the incident laser beam. The Stokes frequency shift is a normal mode of the medium (e.g., vibrational) for SRS, an acoustic frequency for SBS, and the inverse reorientation time of an anisotropic molecule for SRWS. SRS, SBS, and SRWS are resonant phenomena, indicating that the nonlinear medium has a finite response time. In each of these stimulated scattering effects the small-signal gain of the Stokes wave is proportional to the laser intensity.[21]

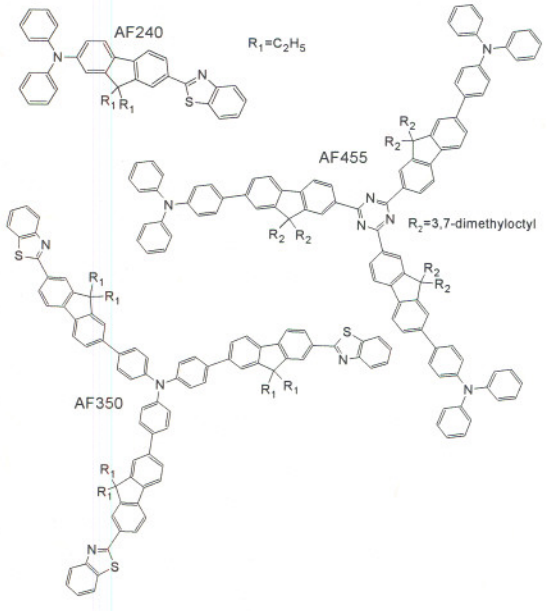

Fig. 1. Chemical structure of AFX molecules used in this study.

The model proposed by He et al. would appear to violate the two conditions previously established for one-way energy transfer by TBC in a Kerr medium. The frequencies are degenerate, and the third order susceptibility related to TPA is due to electronic polarization, which has a virtually instantaneous response for nanosecond laser pulses. Although, under the condition of a TPA resonance, this mechanism may indeed have a finite response time, the intensity dependence of the Kerr effect in TBC is inconsistent with the experimental results reported by He et al.

We have performed detailed nonlinear absorption and photophysical measurements on a system of AFX chromophores and calculate the nonlinear transmission based on an effective three-level model. A numerical model that includes far wing linear absorption has been developed and compared with an analytical three-photon absorption model. The models are in accordance and yield excellent agreement with experimental nonlinear transmission data for 0.02-M AFX solutions up to laser intensities ~ 1 GW/cm^2. Concentration effects at this intensity become increasingly evident. We have extended our modeling efforts to include some new effects that may be anticipated in this regime, such as stimulated scattering, molecular interactions, and saturation. Effects of chirped pulses and linewidth of the pump laser on stimulated scattering are included. We report on our experimental observations of various materials and discuss results with respect to our extended theoretical models.

2. MATERIALS

The chromophores used in this study are part of a class of TPA materials (designated AFX) having a design based on a push-pull charge-transfer model and multi-dimensional conjugation motif.[6] Examples of these molecules are shown in Fig. 1. AF240 is a linear D-π-A chromophore, where the donor (D) is diphenyl-amino and the acceptor (A) is benzothiazole.[6] AF350 is a three-arm octupolar molecule ($D\text{-}A_3$) with a single triarylamino group serving as the electron-rich hub, dialkylfluorenyl bridges, and three π-electron deficient benzothiazoles.[4,22] Except for one less phenyl ring, AF240 is essentially one arm of AF350. AF455 is an $A\text{-}D_3$ type octupolar molecule with 1,3,5-triazine as the hub moiety and diphenylamines as the π-electron donating end-groups.[4] These molecules were synthesized and purified in the Polymer Branch of the Air Force Materials Directorate (AFRL/MLBP) as described in References 4, 6, and 22. Solutions of each were prepared in tetrahydrofuran (THF) for both photophysical characterization and NLT experiments.

A typical linear absorption spectrum is shown in Fig. 2. The λ_{max} is in the UV, with absorption band edges ranging from ~ 450 nm to ~ 470 nm. In each case there is very little absorption ($\sigma_0 < 10^{-21}$ cm^2, see Fig. 2b) in the 2.5-1.4 eV (500-900 nm) region. The energy difference between the absorption band edge and a laser line at 800 nm is ~ 1.5 eV. The purity should be at least 98% for glassy materials (AF-455) and 99% pure for crystalline compounds (AF-240, 350) based on elemental analysis together with spectroscopic methods and melting point determination. There is only a single peak detected by liquid chromatography for both AF-350 and AF-455. An impurity with a peak in the 500-900 nm range with a peak extinction coefficient of ≥10,000 $M^{-1}cm^{-1}$ would be observed at a fractional concentration of 10ppm or less. We conclude that it is unlikely that there is significant impurity absorption in the samples.

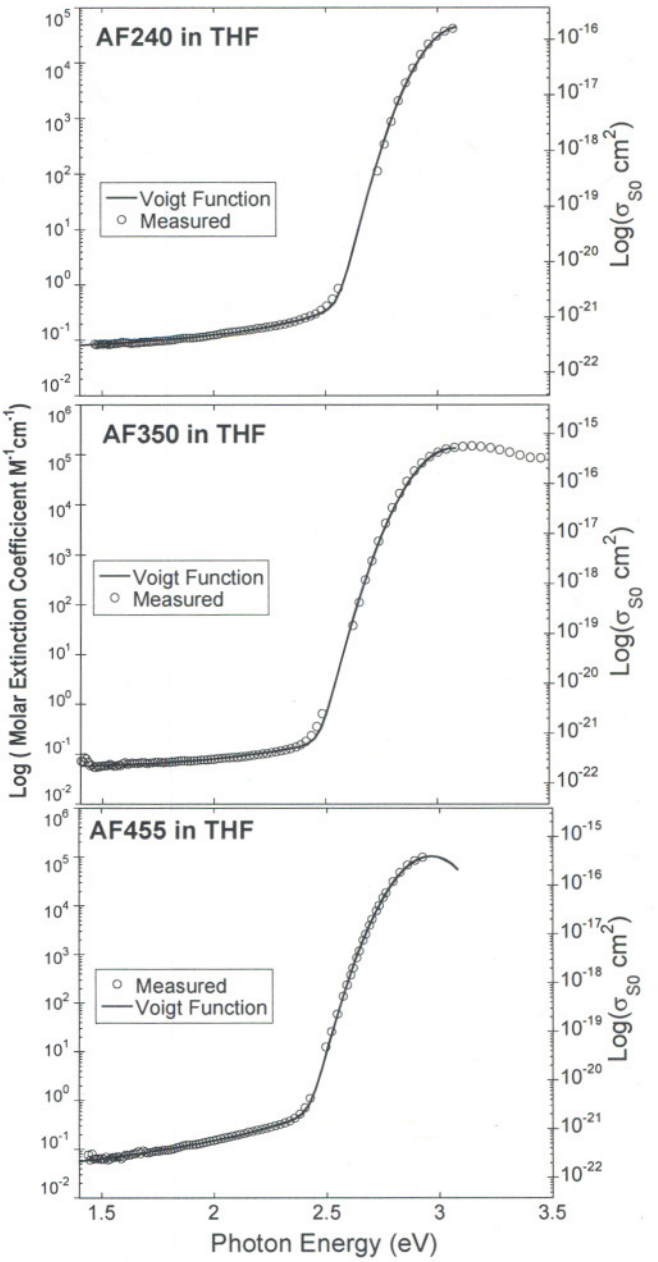

Fig. 2. Linear absorption spectra (ground state cross section σ_0) of AF240, AF350, and AF455 solutions in THF(cicles). The solid lines are a Voigt function fit to the data.

3. THEORETICAL MODELS

3.1. Effective TPA and 3PA Models

We seek a simple analytical model that can adequately explain and reliably predict, within a reasonable degree of approximation, the nanosecond NLT based on measurable properties of the chromophores and the laser pulse. This model is similar to that used for reverse saturable absorption media, but with TPA from the ground state.[23] We consider ESA from the lowest lying singlet and triplet states. Two-photon-induced ESA is a three-photon process, although three photons are not absorbed simultaneously due to the finite lifetimes of the excited states. It is of interest, nevertheless, to see how useful a three-photon absorption

(3PA) model is in explaining the data. In the following we present the conditions and approximations for employing such a model.

With the above assumptions, we have for the intensity I,

$$\frac{\partial I}{\partial z} = -(\beta + \gamma I) I^2 \tag{1}$$

where

$$\gamma = \frac{\tau_p \sigma_{eff} \sigma_2 N}{2\hbar\omega}, \tag{2}$$

$$\sigma_{eff} = \eta \sigma_{S1} + \left(\tfrac{1}{2} - \eta\right) \varphi_T \sigma_{T1}, \tag{3}$$

and $\beta = \sigma_2 N$ is the TPA coefficient. We have thus modeled the system as a two-photon resonant, three-photon absorption medium, with an effective intermediate state that represents a time-averaged combination of the S_1 and T_1 states. Several authors have taken the quantity in parentheses in Eq. (1) to represent an effective TPA coefficient β_{eff}, from which an effective TPA cross section can be derived. We will consider both effective TPA and 3PA models in analyzing the experimental data. The quantity η is the pulse-averaged, relative weight of the S_1 state contribution to the effective ESA cross section. When $\tau_p << \tau_S$, $\eta \approx ½$ and ESA is essentially from the S_1 state only. On the other hand, when $\tau_p >> \tau_S$, $\eta \approx 0$ and all ESA is effectively from the T_1 state. When $\tau_p << \tau_S$, the growth of the S_1 population is linear, and the average growth time over a rectangular pulse is just $\tau_p/2$. The maximum relative weight of ½ for either state reflects the fact that in either time regime the growth rate of the respective excited state population (singlet or triplet) is approximately constant. The average population density over the entire pulse is then just one-half of the maximum density obtained at the end of the pulse, $N_{S1,max} = \varphi_T^{-1} N_{T1,max} = \tau_p \sigma_2 N I_{peak}^2 / 2\hbar\omega$. In an intermediate regime where $\tau_T >> \tau_p$ and $\tau_p \sim \tau_S$, $\eta < ½$ means that the S_1 population at the end of the pulse is smaller than $N_{S1,max} \sim N_{S1}^{ss}$ because of continuous transitions to the S_0 and T_1 states as S_1 is being pumped, analogous to a leaky capacitor.

Equation (1) can be solved analytically, but the resulting expression is transcendental. However, if we take $\beta << \gamma I$, the result reduces to a simple closed form identical to that for three-photon absorption. Assuming now Gaussian spatial and temporal profiles for the incident intensity, we integrate the resulting expression over space and time to obtain the energy transmittance for a sample of thickness d:

$$T = \frac{T_0^2}{\sqrt{\pi}\, p_0} \int_{-\infty}^{+\infty} \ln\left[\sqrt{1 + p_0^2 \exp\left(-2x^2\right)} + p_0 \exp\left(-x^2\right)\right] dx \tag{4}$$

where T_0 is the net linear transmittance from air into the medium due to Fresnel losses only (including all dielectric interfaces), $p_0 = (2\gamma T_0^2 I_0^2 d)^{1/2}$, and I_0 is the incident peak, on-axis intensity.[24] The parameters determining γ can be found from femtosecond, picosecond, and nanosecond photophysical measurements and standard TPA measurements in the femtosecond regime.

3.2. Numerical ESA Model

The numerical model calculates the spatial, time, and radial dependence of three state populations; all of the transitions between these states; the bimolecular processes of triplet-triplet annihilation, ground state quenching, and oxygen quenching. The radiation transport equation is then,

$$\frac{\partial I}{\partial z} = -\sigma_{S0} N_{S0} I - \sigma_2 N_{S0} I^2 - \sigma_{S1} N_{S1} I - \sigma_{T1} N_{T1} I \tag{5}$$

The population rate equations are,

$$\frac{\partial N_{S0}}{\partial t} = -\frac{I}{\hbar\omega}\left(\sigma_{S0} + \frac{\sigma_2 I}{2}\right)N_{S0} + \left(\frac{1-\varphi_T}{\tau_S}\right)N_{S1} + \left(\frac{1}{\tau_T} + \frac{\kappa_{TT}}{2}N_{T1} + \kappa_{ST}N_{S0} + \kappa_{OT}N_O\right)N_{T1} \tag{6a}$$

$$\frac{\partial N_{S1}}{\partial t} = \frac{I}{\hbar\omega}\left(\sigma_{S0} + \frac{\sigma_2 I}{2}\right)N_{S0} - \frac{N_{S1}}{\tau_S} + \frac{\kappa_{TT}}{2}N_{T1}{}^2 \tag{6b}$$

$$\frac{\partial N_{T1}}{\partial t} = \frac{\varphi_T}{\tau_S}N_{S1} - \left(\frac{1}{\tau_T} + \frac{\kappa_{TT}}{2}N_{T1} + \kappa_{ST}N_{S0} + \kappa_{OT}N_O\right)N_{T1} \tag{6c}$$

$$\frac{\partial N_O}{\partial t} = -\kappa_{OT}N_O N_{T1} + k_O\left(N_O^0 - N_O\right) \tag{6d}$$

$$N_{S0} = N - N_{S1} - N_{T1}\,. \tag{6e}$$

where κ_{TT}, κ_{ST}, κ_{OT}, N_O, k_O are the triplet-triplet annihilation rate, the ground state self quenching rate of the triplet state, the oxygen quenching rate of the triplet state, the oxygen concentration, and the oxygen singlet state relaxation rate respectively. The rate equations are solved using a stiff Runge-Kutta algorithm supplied in MathCad. This requires the Jacobian to be supplied which was derived. This is solved at every time step. These populations are used to calculate the change in the intensity which is then rescaled assuming Gaussian beam propagation at each z step. A range of input intensities are calculated and used to calculate both the NLT variation and the radial dependence. A Gaussian time profile is used since the measured laser profile nearly matches a Gaussian. The radial and temporal integrations are done to give transmitted pulse energy and compared to the measured data. A normal reflection Fresnel loss is imposed on the incident intensity and again on the output intensity. A refractive index of 1.4535 is used for fused silica at 800 nm and 1.511 for BK7 at 800 nm. The Fresnel reflection at the glass liquid interface is found to be negligible and is not included.

3.3. Stimulated Scattering Model

Consider a field with a time dependent amplitude and phase, $E(t) \sim A(t)\exp[-i\varphi(t)]$. A Taylor series expansion of the phase yields (ignoring a constant term) $\varphi(t) = \omega t + bt^2 + \ldots$, where ω is the central frequency of the wave, and b is a linear chirp coefficient. For simplicity, I will ignore higher order terms. Co-propagating TBC with chirped pulses has been examined in Kerr media with a finite response time.[25-27] However, none of these previous studies have considered the interaction of counter-propagating waves through TPA-populated excited states.

Let the total field in a medium of length d be described by

$$\begin{aligned} E(z,t) = {} & A_L(z,t+\tau)\exp\left\{i[kz - \omega t - b(t+\tau)^2]\right\} \\ & + A_S(z,t-\tau)\exp\left\{i[-kz - \omega t - b(t-\tau)^2]\right\} + c.c. \end{aligned} \tag{7}$$

where $k = n\omega/c$, n is the linear refractive index, and $2\tau = 2n(d-z)/c$ is the relative time delay at position z and time t between the forward propagating laser wave (L) and the backward propagating scattered wave (S). I assume that the scattered wave originates at $z = d$ by some elastic scattering process, so $A_S(d,t) = \sqrt{\eta}\,A_L(d,t)$ where η is a constant << 1. Consequently, the scattered wave has the same spectral composition as the incident laser wave. However, for $z \neq d$ a lower frequency part of the scattered wave is always interacting with a higher frequency part of the incident wave. The total polarization of the medium is given by

$$P = \varepsilon_0\left(\chi_g^{(1)} + (N_e/N)\Delta\chi^{(1)} + 3\chi^{(3)}\left\langle E^2\right\rangle\right)E \tag{8}$$

where $\chi^{(n)}$ is the n-th order susceptibility, and the angular brackets indicate an average over a time longer than an optical period but shorter than $(2b\tau)^{-1}$. We have assumed that TPA produces a single excited state of number density N_e << N, the total number density of the nonlinear chromophore. We have also assumed an isotropic medium with linearly polar-

ized light for simplicity, and both $\Delta\chi^{(1)} = \chi_e^{(1)} - \chi_g^{(1)}$ and $\chi^{(3)}$ are complex quantities (g signifies the ground state of the medium). The excited state decays back to the ground state with a time constant T_e, so N_e obeys the following kinetic equation:

$$\frac{\partial N_e}{\partial t} = \frac{\sigma_2 N I^2}{2\hbar\omega} - \frac{N_e}{T_e} \tag{9}$$

where $\sigma_2 = \beta/N$ is the TPA cross section (β is the TPA coefficient), and $I(z,t) = 2\varepsilon_0 nc\langle E^2(z,t)\rangle$ is the total intensity. Let the amplitudes be slowly varying in time compared to T_e. Equation (9) can then be integrated to yield

$$N_e/N = C_0 + \{C_1 \exp[i(2kz - 4b\tau t)] + C_2 \exp[i(4kz - 8b\tau t)] + c.c.\}, \tag{10a}$$

$$C_0 = \frac{\sigma_2 T_e}{2\hbar\omega}\left(I_L^2 + I_S^2 + 4I_L I_S\right), \tag{10b}$$

$$C_1 = \frac{\sigma_2 T_e}{2\hbar\omega}(I_L + I_S)\left(\frac{4\varepsilon_0 ncA_L A_S^*}{1 - i4b\tau T_e}\right), \tag{10c}$$

$$C_2 = \frac{\sigma_2 T_e}{2\hbar\omega}\frac{\left(2\varepsilon_0 ncA_L A_S^*\right)^2}{1 - i8b\tau T_e}, \tag{10d}$$

where ε_0 is the free-space permittivity. We will make the assumption that $(4b\tau T_e)^2 << 1$.

Following a procedure directly analogous to that of Yeh[20] and Boyd[21] for non-degenerate TBC, Eqs. (10a)-(10d) are substituted into Eq. (8), and then both Eqs. (7) and (8) are substituted into Maxwell's wave equation in the slowly varying amplitude approximation. Matching up synchronous terms, the following coupled-wave equations for the laser and backscattered intensities are derived:

$$\frac{dI_L}{dz} = -g(1 - z/d)(I_L + I_S)I_L I_S - \gamma_{eff}\left(I_L^2 + 3I_S^2 + 6I_L I_S\right)I_L - \beta(I_L + 2I_S)I_L \tag{11a}$$

$$\frac{dI_S}{dz} = -g(1 - z/d)(I_L + I_S)I_L I_S + \gamma_{eff}\left(3I_L^2 + I_S^2 + 6I_L I_S\right)I_S + \beta(2I_L + I_S)I_S \tag{11b}$$

where g and γ_{eff} are the backward wave gain and effective three-photon absorption (3PA) coefficients, respectively, with

$$g = \frac{8bT_e\omega\Delta\chi_R^{(1)}d}{c^2 I_{sat}^2}, \tag{12}$$

$$\gamma_{eff} = \frac{N\Delta\sigma}{I_{sat}^2}, \tag{13}$$

where $\Delta\chi_R^{(1)} = \mathrm{Re}\left(\Delta\chi^{(1)}\right)$, $\Delta\sigma = \sigma_e - \sigma_g$ is the difference between the linear absorption cross sections of the excited and ground states, and $I_{sat} = (2\hbar\omega/\sigma_2 T_e)^{1/2}$ is the two-photon saturation intensity. Note that $g = 0$ when $b = 0$ (no chirp). Hence, without chirp there can be no growth of the backward scattered wave. The gain g also carries the sign of b (positive or negative chirp). For a negatively chirped pulse, the scattered wave will be attenuated. For the rest of the paper, we will assume that $b > 0$.

4. EXPERIMENTAL

Micromolar solutions were prepared for conventional photophysical measurements (lifetimes, excited state cross sections, and quantum yields). Details of these experiments can be found elsewhere.[23] All solution samples for nanosecond NLT measurements had concentrations of 0.02 M (mol/L) and were placed in 1-mm glass or fused silica cuvettes. Intrinsic σ_2 values were obtained from independent femtosecond measurements.[23-25]

Nanosecond nonlinear transmittance measurements were performed with a Nd:YAG pumped optical parametric oscillator (OPO) tuned from 660 to 880 nm. The pulse was Gaussian shaped with τ_L = 3.2 ns. The beam was focused with an f = 50-cm lens into the sample. Over the length of the sample (1 mm) the beam was essentially collimated. The beam shape was slightly elliptical, with a geometric-mean $1/e^2$ radius $w \approx 18.4 - 18.9$ μm, assuming an approximately Gaussian beam shape. The energy was varied, and incident and transmitted energies were measured with energy meters. To rule out the effects of self-focusing/defocusing, a large-area (~ 1 cm^2) detector was placed near the exit of the sample to collect all transmitted energy. We also looked for stimulated backscattering by rotating the sample slightly to avoid Fresnel reflected light and measuring 180°-scattered light with an energy meter.

Intermolecular quenching properties were examined. The ground state concentration was varied from 10 μM to 20 mM, and the triplet state lifetime measured. At ~ 10 μM the lifetime of AF350 was 182 μs under deoxygenated conditions, and the lifetime was 96μs at 20 mM. A bimolecular self-quenching rate constant of 2×10^2 $M^{-1}s^{-1}$ was measured The NLA experiments were performed under air-saturated conditions, and this small amount of quenching will make no difference since it is in competition with oxygen quenching. Similarly, AF350 run at low and high energy excitation conditions produced no measurable change in the decay rate attributable to triplet-triplet annihilation. This is not unexpected due to the low triplet yield of these materials. Due to the similarity of these materials in structure and known triplet yield, we assume that these intermolecular processes do not play a significant role at this concentration.

5. RESULTS AND DISCUSSION

A common method in the literature for screening TPA materials in the nanosecond regime is to fit the NLT data to an effective TPA transmittance (see Eq. (1)) and extract an effective TPA cross section. We show the results of such fits for two series of dipolar (AF240 and AF 270), quadrupolar (AF287 and AF295), and octupolar (AF380 and AF350) molecules in Table 1. Another series of chromophores have been measured at a variety of wavelengths, and their effective TPA cross sections are given in Table 2. Such data are useful for observing trends, in molecular structure and spectrally, but do not yield sufficient information to give directions for further improvement. For example, a large effective σ_2 could be due to a large intrinsic σ_2, a large singlet and/or triplet cross section, and/or a large triplet yield. Hence, these NLT measurements must be supplemented with photophysical measurements. Both effective 3PA and numerical ESA models may then be applied to ascertain the quality of the model in reproducing the NLT results.

Table 1. Effective TPA Cross Sections of a Series of AFX Chromophores

Material	File	Eff σ_2 (10^{-20} cm^4/GW)
AF240	NLA 130	50
AF287	NLA 134	99
AF380	NLA 131	114
AF270	NLA 132	29
AF295	NLA 136	78
AF350	NLA 137	139

Table 2. Spectral Effective TPA Cross Sections for Four Chromophores

Chromophore	File	Eff σ_2 (10^{-20} cm^4/GW)	λ (nm)
AF445	NLA0841	44	660
	NLA0771	103	740
	NLA0804	29	800
	NLA0816	8	880
E1-BTF	NLA0842	195	660
	NLA0756	145	740
	NLA0801	80	800
	NLA0817	0	880
AF380-118	NLA0847	67	660
	NLA0761	117	740
	NLA0807	69	800
	NLA0822	100	880
IR-2	NLA0850	114	660
	NLA0776	98	740
	NLA0809	103	800
	NLA0825	185	880

Results of NLT measurements for 0.02-M solutions of AF455, AF350, and AF240 in THF are given in Figs. 3-5, respectively. Using sets of intrinsic σ_2 values, we calculated the NLT for each material and compare these calculations to the data in Figs. 3-5. Only experimental data were used in the calculations; there were no adjustable parameters.

In Fig. 3 there is good agreement between theory and experiment when the value of $\sigma_2 = 0.51 \times 10^{-20}$ cm^4/GW is used. This value was obtained in a femtosecond NLT experiment[30] for a 0.02-M solution of AF455 in THF, identical to the sample studied here. Although the wavelength used in that experiment was 790 nm, the TPA spectrum[4] indicates that σ_2 does not differ significantly at 800 nm, considering the experimental uncertainty of ±15%.

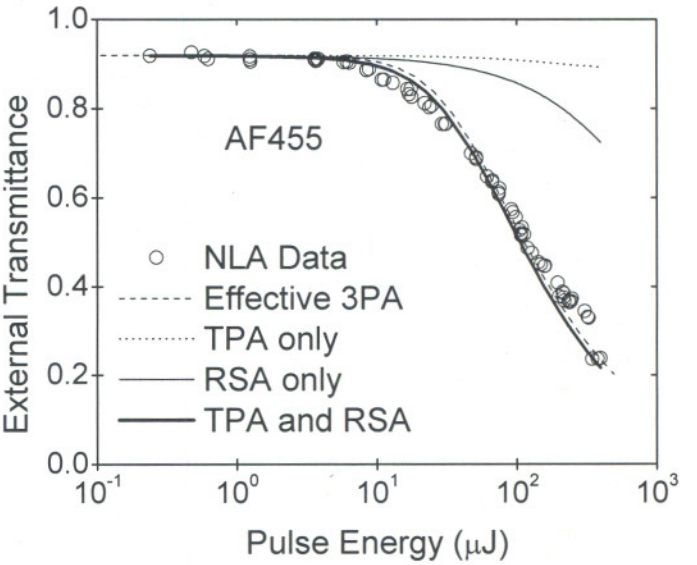

Fig. 3. Experimental (circles) and theoretical (curves) nanosecond nonlinear transmittance as a function of laser pulse energy for a 0.02-M THF solution of AF455 at 800 nm. The curves are for the analytical effective three-photon absorption model, the numerical model with only TPA driving excitation, with only the ground state driving excitation (labeled RSA) and for the complete system.

Figure 3 also compares the transmittance in AF455 calculated for two-photon induced ESA (effective 3PA analytical model) with that due to TPA alone (numerical), and reverse saturable absorption (RSA) which includes the ground state absorption and excited state absorption. Obviously, ESA is the dominant loss mechanism. The inclusion of ground state absorption gives rise to significant nonlinear absorption and fits the data more closely in the region near < 10 μJ where these models are the most reliable.

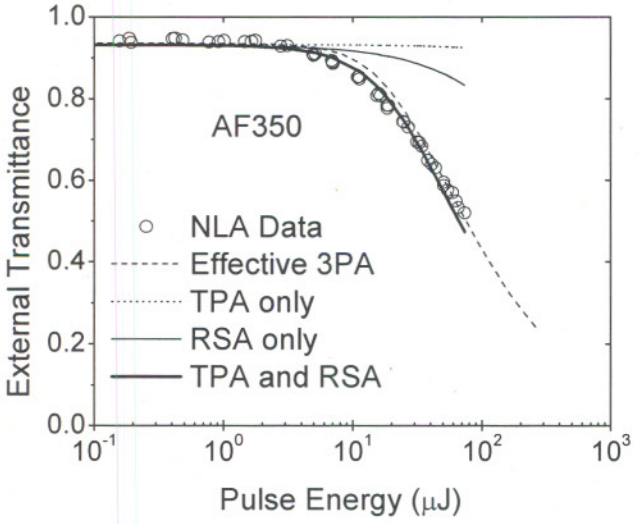

Fig. 4. The curves are as described in Figure 10 but for a 0.02-M THF solution of AF350 at 820 nm

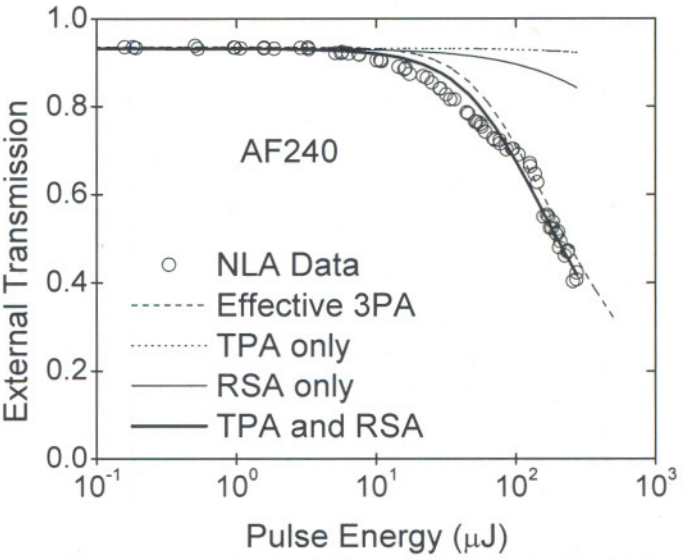

Fig. 5. The curves are as described n Figure 10 but for a 0.02-M THF solution of AF240 at 820 nm..

We note for all materials that there is some departure of experiment from theory in the low energy regime (~ 10 μJ). It is interesting that an effective TPA theory fits the data better in this regime, indicating that some mechanism that has a quadratic intensity dependence may be at play. He et al.[17] have observed this kind of dependence and have verified in their case that this is due to a stimulated scattering phenomenon. We consider this next.

Let us examine Eqs. (11a) and (11b) in the case when $I_S << I_L \approx$ constant. It can be seen that the backward stimulated wave will experience exponential growth when $I_L > 2\beta/\left(\frac{1}{2}g - 3\gamma_{eff}\right)$. This defines the threshold condition for stimulated backscattering when there is no linear absorption. From Eq. (11b), the small signal gain G, given in terms of $\Delta I_S = I_S(0) - I_S(d)$, is $G = \Delta I_S / I_S(d) \propto I_L^2$ for input intensities where the gain dominates TPA. Also, the reflectance of the scattered wave is defined by $R = I_S(0)/I_L(0)$, and the change $\Delta R = R - \eta = \Delta I_S / I_L \propto I_S(d) I_L \propto G I_S(d)/I_L$. These results are in agreement with the data presented by He et al. for the measured small-signal gain and reflectance in a 0.01-M solution of PRL 802 in THF.[17]

Under conditions where the nonlinear absorption terms (β and γ_{eff}) can be ignored, Eqs. (11a) and (11b) can be solved analytically. The result can be expressed as

$$\eta_0 = \frac{R\left[(1-R)(1-R+3\eta_0)+2\eta_0^2\right]^{1/2}}{(1+R)^2\exp(\Gamma)}\left(\frac{1-R+2\eta_0}{1-R+\eta_0}\right)^{3/2}, \tag{14}$$

where $\eta_0 = I_S(d)/I_L(0)$, and

$$\Gamma = \tfrac{1}{2}(1-R)^2 g I_L^2(0) d. \tag{15}$$

Note that in general $\eta_0 \neq \eta$, although when the gain is sufficiently small $\eta_0 \approx \eta$. Also, when the gain is not too large so that $(1 - R) >> \eta_0$, Eq. (14) can be simplified to the following approximation:

$$\eta_0 \approx \frac{R(1-R)}{(1+R)^2\exp(\Gamma)}. \tag{16}$$

It is interesting to compare this result to the case of SBS, for which the denominator of Eq. (16) becomes $\exp(\Gamma) - R$ with $\Gamma \to (1-R) g_B I_L(0) d$, where g_B is the Brillouin gain coefficient.[21] Thus, in the case of negligible loss by absorption, the backscattered reflectance as a function of incident laser intensity will look similar to the Brillouin reflectance. A plot

of the reflectance given by Eq. (16) for a constant input $I_S(d)/I_L(0)$, over a range of Γ where the approximation is valid, is shown in Fig. 6.

Numerical solutions of Eqs. (11a) and (11b) are also given in Fig. 6. These illustrate the agreement of the approximation given by Eq. (16) with the exact result, and the effect of including the nonlinear absorption terms. Figure 7 gives $I_S(0)$ as a function of $I_L(0)$. Parameters have been adjusted to yield results close to the experimental data of He et al.[16,17] The coefficients used for the solid curve in Fig. 7 are $\beta = 9.46$ cm/GW (the value quoted in Ref. 17), $\eta = 0.04$, $g = 1800$ cm^3/GW^2, and $\gamma_{eff} = 120$ cm^3/GW^2, with $d = 1$ cm. In Fig. 8 the corresponding plot for the laser transmittance is given. Here the transmittance is the ratio of output power to input power. To compute this, we assumed a Gaussian dependence for the input intensity and then integrated the output intensity over the area of the cylindrically symmetric beam. The result is compared with what would be expected for pure TPA (no TBC or ESA). The departure from pure TPA in this case is due primarily to energy transfer from the laser to the backscattered beam. Figure 7 also shows a somewhat different result (dashed curve) yielding comparable backscattered intensity. Often the effective TPA cross section measured in the nanosecond regime is a factor ~ 100 larger than the intrinsic cross section (usually measured in the femtosecond regime).[31] Thus, for these calculations we chose $\beta = 0.09$ cm/GW. The other parameters are $\eta = 0.02$, $g = 2860$ cm^3/GW^2, and $\gamma_{eff} = 300$ cm^3/GW^2. TPA is low in this case, but the loss due to ESA significantly slows down the growth of the backscattered wave at higher intensities.

To get an order of magnitude of the numbers involved, consider the experiment of He et al.[16,17] and the results shown in Figs. 7 and 8 for $\beta = 9.46$ cm/GW. For a laser wavelength of 532 nm and $T_e \sim 1$ ns,[5,31] $I_{sat} \sim 700$ MW/cm^2. For a severely chirped pulse the laser linewidth is $\Delta\omega_L \sim 2b\tau_L$ where τ_L is the laser pulse width. For $\Delta\omega_L/2\pi \sim 24$ GHz (0.8 cm^{-1}), $\tau_L \sim 10$ ns, and $N = 6 \times 10^{18}$ cm^{-3} (0.01-M concentration), Eqs. (12) and (13) yield $\Delta\chi_R^{(1)} \sim 4 \times 10^{-3}$ and $\Delta\sigma \sim 1 \times 10^{-17}$ cm^2. We note that this numerical example contravenes the approximation made earlier for which $(4b\tau T_e)^2$ is small compared to 1. To account for deviations due to this, the gain and ESA terms in Eqs. (11a) and (11b) would need to be modified by the inclusion of the factor $[1 + (4b\tau T_e)^2]^{-1}$. For example, in the negligible nonlinear absorption case, Eq. (16) would be multiplied by a factor $\ln(1 + \alpha)/\alpha$, where $\alpha = (4bT_e nd/c)^2$, which is ~ 1 for $\alpha << 1$. In the present numerical example, this factor is ~ 0.5. Consequently, the estimates for $\Delta\chi_R^{(1)}$ and $\Delta\sigma$ should be increased by a factor ~ 2. These values yield approximate agreement with photophysical measurements, and thus suggests that this stimulated scattering with a quadratic intensity dependence may be contributing to the overall shape of the NLT curve.

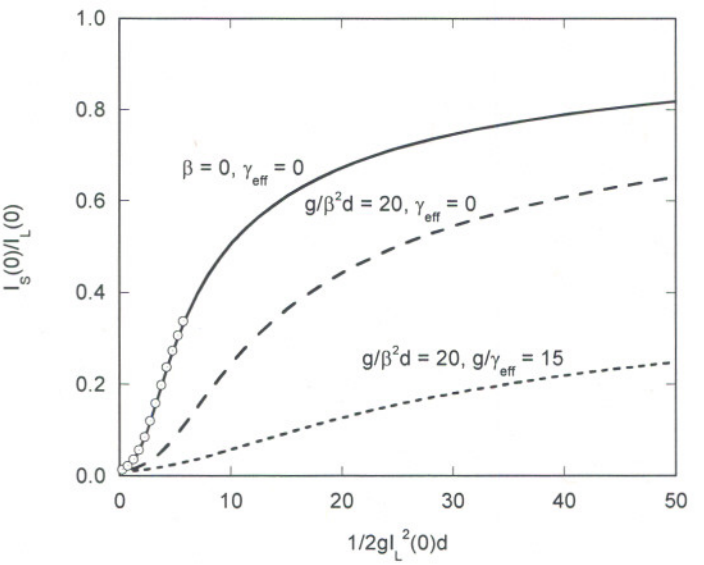

Fig. 6. Backscattered reflectance as a function of exponential gain factor for various values of nonlinear absorption coefficients. $I_S(d)/I_L(0) = 10^{-2}$ in all cases. Circles give values for R calculated by the approximation in Eq. (10).

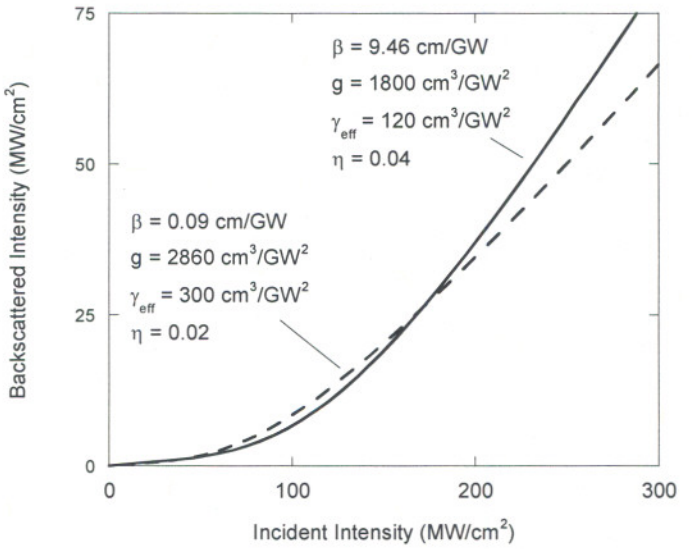

Fig. 7. Backscattered intensity as a function of incident laser intensity.

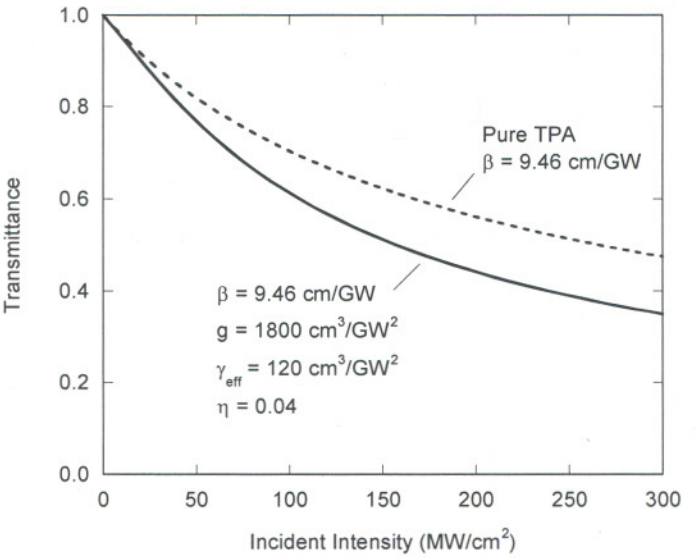

Fig. 8. Nonlinear transmittance of the incident laser as a function of incident intensity.

Notice that $\mathrm{Re}\left(\chi^{(3)}\right)$, or n_2, does not appear in the gain coefficient of Eq. (12). The reason for this is that $\chi^{(3)}$ was assumed to have an instantaneous response [$\mathrm{Im}\left(\chi^{(3)}\right) \propto \beta$]. There is no two-beam coupling in a Kerr medium with an instantaneous response.[20,21] It is possible however, under TPA resonant conditions, that n_2 could have a finite response time (i.e., $\chi^{(3)}$ is complex with a finite damping coefficient[21]). However, if this is included in the development of the coupled-wave intensity equations, it would lead to a term in the gain G that is proportional to I_L, not I_L^2, which would be inconsistent with the experimental results of He et al.[17] It is also quite likely that the Kerr refractive term would be much smaller than the term proportional to $\Delta\chi_R^{(1)}$.

The central feature of this theory is contained in the term $4b\tau T_e \equiv \Delta\omega T_e$, where $\Delta\omega = 4b\tau$ represents the instantaneous difference in the frequency between the forward and backward propagating waves at position z in the medium. $\Delta\omega$ varies continuously from 0 at $z = d$ to a maximum of $4bnd/c$ at $z = 0$. The interference of the forward and backward propagating waves sets up an interference pattern that is traveling to the left if $b > 0$. This intensity pattern forms a population grating via TPA, which lags behind the interference pattern due to the finite response time T_e. By examining Eqs. (10c),

(10a), and (8), we see that $\Delta\omega T_e \neq 0$ results in a contribution to the imaginary part of the total refractive index of the medium due to the presence of the two waves. As Boyd has observed in the context of nondegenerate TBC in a Kerr medium, the only way to obtain a complex refractive index (apart from pure absorption), and thus to achieve energy coupling between the two waves, is that the product $\Delta\omega T_e$ not vanish.[21] In the present theory, this requires a non-zero chirp ($b \neq 0$). This can also be explained by considering the phase difference $\Delta\varphi = 4b\tau T_e$ between the polarization and the field. The rate of energy transfer per unit volume to or from an electric field E by a polarization P is $2\mathrm{Re}[i\omega|E||P|\exp(i\Delta\varphi)]$, which is 0 if $\Delta\varphi = 0$.[32] Thus, although backscattering by an unchirped wave could also lead to a population grating, the grating would not transfer energy to the scattered wave because the field and polarization would be in phase. There would thus be no increase in the index modulation as the incident intensity increases and no exponential growth of the scattered wave, i.e., no stimulated scattering. This has an analogy in SBS and SRS. In both cases, the gain is related to the imaginary part of the nonlinear susceptibility, which vanishes when the difference between the laser and scattered wave frequencies shrinks to zero. In addition, the scattered wave in the present theory is attenuated for a negative chirp, analogous to the attenuation of the anti-Stokes wave in SBS and SRS.[21]

It should be noted at this stage that linear chirp is not a unique requirement for the energy transfer between incident laser and elastically backscattered waves. Higher order chirp terms in the nonlinear time dependent phase have been ignored for simplicity but will make additional contributions to the beam coupling. Another potential mechanism involves multimode beams. In this case, though, the spectral nature of the backscattered beam will not match that of the incident beam. Take the simple case where the incident laser wave consists of two modes: ω_0 and $\omega_1 = \omega_0 + \delta\omega > \omega_0$ ($\delta\omega << \omega_0$). Employing the mechanism involving a TPA-populated excited state described above, there will be energy transfer from the ω_1 mode of the incident laser beam to the ω_0 mode of the backscattered beam.[21] Likewise, the ω_1 mode of the backscattered wave will yield its energy to the ω_0 mode of the laser wave. The backscattered wave will thus be single-mode and its spectrum conspicuously different from the incident laser. However, if the modes in the incident laser beam are equally chirped, both modes of the backscattered wave will be amplified, but not equally. When the laser linewidth is determined primarily by the linear chirp ($2b\tau_L >> \delta\omega$), the spectrum of the backscattered wave will superficially resemble that of the incident laser, but the energy distribution amongst the modes will differ. This will generally be the case also when the number of modes is greater than two. Scattering due to multimode effects have not been studied to any large extent. We plan to further examine this both theoretically and experimentally.

6. CONCLUSIONS

In summary, we have measured the excited state properties of donor-acceptor push-pull charge-transfer chromophores and modeled the nanosecond NLT as an effective three-photon absorption process combined with stimulated scattering at high intensities. All model parameters, including intrinsic TPA cross sections, have been measured independently, and the model agrees very well with much of the experimental data for those values of femtosecond TPA cross sections that were measured under conditions similar to those of our experiments. A numerical calculation that includes the ground state absorption gives significantly better fit to the NLT data. These calculations have no adjustable parameters. A careful examination of linear absorption data gives evidence for a two-step TPA via the Lorentzian tail between the S_0 and S_1 states. We conclude that the dominant contribution to the nonlinear transmission in these chromophores in the nanosecond regime is ESA from both singlet and triplet states. TPA does not contribute significantly to the transmittance loss, but is key to pumping the excited states. We expect that this is true for a large variety of these types of chromophores. We have also presented a model of two-beam coupling in a nonlinear absorption medium whereby energy is transferred from an incident laser beam to an elastically backscattered beam. In the mechanism proposed, the incident laser has a nonlinear time dependent phase and populates an excited state of the medium by two-photon absorption. The incident and backscattered waves superpose to form an interference pattern, leading to the formation of a Bragg grating. The Bragg grating consists of an index modulation resulting from a modulation of the excited state population. This grating is out of phase with the interference pattern which forms it due to the finite lifetime of the two-photon-populated excited state and the frequency chirp of the two waves. Energy flows one-way from the higher frequency part to the lower frequency part of the coupled waves. Complete energy conversion to the backscattered wave is prohibited, however, in part because of loss due to two-photon and excited state absorption. Nevertheless, the power spectrum of the backscattered wave can be nearly identical to that of the incident wave. This mechanism may be at work and explain the NLT curves at lower intensities near energies of 10 μJ.

ACKNOWLEDGEMENTS

We gratefully acknowledge the Air Force Office of Scientific Research (AFOSR/NL) for their support of this work, as well as support from AFRL/ML.

REFERENCES

1. M. Albota, D. Beljonne, J. –L. Brédas, J. E. Ehrlich, J. –Y. Fu, A. A. Heikal, S. E. Hess, T. Kogej, M. D. Levin, S. R. Marder, D. McCord-Maughon, J. W. Perry, H. Röckel, M. Rumi, G. Subramaniam, W. W. Webb, X. –L. Wu, and C. Xu, "Design of organic molecules with large two-photon absorption cross sections," Science 281, 1653-1656 (1998).
2. B. A. Reinhardt, L. L. Brott, S. J. Clarson, A. G. Dillard, J. C. Bhatt, R. Kannan, L. Yuan, G. S. He, and P. N. Prasad, "Highly active two-photon dyes: Design, synthesis, and characterization toward application," Chem. Mater. **10**, 1863-1874 (1998).
3. M. Rumi, J. E. Ehrlich, A. A. Heikal, J. W. Perry, S. Barlow, Z. Hu, D. McCord-Maughon, T. C. Parker, H. Röckel, S. Thayumanavan, S. R. Marder, D. Beljonne, and J. –L. Brédas, "Structure-property relationships for two-photon absorbing chromophores: bis-donor diphenylpolyene and bis(styryl)benzene derivatives," J. Am. Chem. Soc. **112**, 9500-9510 (2000).
4. R. Kannan, G. S. He, T. –C. Lin, P. N. Prasad, R. A. Vaia, and L. –S. Tan, "Toward highly active two-photon absorbing liquids. Synthesis and characterization of 1,3,5-triazine-based octupolar molecules," Chem. Mater. **16**,185-194 (2004).
5. J. E. Ehrlich, X. –L. Wu, I. –Y. S. Lee, Z. –Y. Hu, H. Röckel, S. R. Marder, and J. W. Perry, "Two-photon absorption and broadband optical limiting with bis-donor stilbenes," Opt. Lett. **22**, 1843-1845 (1997).
6. R. Kannan, G. S. He, L. Yuan, F. Xu, P. N. Prasad, A. G. Dombroskie, B. A. Reinhardt, J. W. Baur, R. A. Vaia, and L. –S. Tan, "Diphenylaminofluorene-based two-photon-absorbing chromophores with various π-electron acceptors," Chem. Mater. **13**, 1896-1904 (2001).
7. J. Kleinschmidt, S. Rentsch, W. Tottleben, and B. Wilhelmi, "Measurement of strong nonlinear absorption in stilbene-choloform solution, explained by the superposition of two-photon absorption and one-photon absorption from the excited state," Chem. Phys. Lett. **24**, 133-135 (1974).
8. M. Zhao, Y. Cui, M. Samoc, P. N. Prasad, M. R. Unroe, and B. A. Reinhardt, "Influence of two-photon absorption on third-order nonlinear optical processes as studied by degenerate four-wave mixing: The study of soluble didecyloxy substituted polyphenyls," J. Chem. Phys. **95**, 3391-4401 (1991).
9. R. L. Sutherland, E. Rea, L. V. Natarajan, T. Pottenger, and P. A. Fleitz, "Two-photon absorption and second hyperpolarizability measurements in diphenylbutadiene by degenerate four-wave mixing," J. Chem. Phys. **98**, 2593-2603 (1993).
10. P. Palffy-Muhoray, H. J. Yuan, L. Li, M. A. Lee, J. R. DeSalvo, T. H. Wei, M. Sheik-Bahae, D. J. Hagan, and E. W. Van Stryland, "Measurements of third order optical nonlinearities of nematic liquid crystals," Mol. Cryst. Liq. Cryst. **207**, 291-305 (1991).
11. A. A. Said, C. Wamsley, D. J. Hagan, E. W. Van Stryland, B. A. Reinhardt, P. Roderer, and A. G. Dillard, "Third- and fifth-order optical nonlinearities in organic materials," Chem. Phys. Lett. **228**, 646-650 (1994).
12. S. Guha, K. Kang, P. Porter, J. F. Roach, D. E. Remy, F. J. Aranda, and D. V. G. L. N. Rao, "Third-order optical nonlinearities of metallotetrabenzoporphyrins and a platinum poly-yne," Opt. Lett. **17**, 264-266 (1992).
13. D. A. Oulianov, I. V. Tomov, A. S. Dvornikov, and R. M. Rentzepis, "Observations on the measurement of two-photon absorption cross-section," Opt. Commun. **191**, 235-243 (2001).
14. J. Swiatikiewicz, P. N. Prasad, and B. A. Reinhardt, "Probing two-photon excitation dynamics using ultrafast laser pulses," Opt. Commun. **157**, 135-138 (1998).
15. F. Gel′mukhanov, A. Baev, P. Macák, Y. Luo, and H. Ågren, "Dynamics of two-photon absorption by molecules and solutions," J. Opt. Soc. Am. B **19**, 937-945 (2002).
16. G. S. He, T. –C. Lin, and P. N. Prasad, "Stimulated Rayleigh-Bragg scattering enhanced by two-photon excitation," Opt. Express **12**, 5952-5961 (2004).
17. G. S. He, C. Lu, Q. Zheng, P. N. Prasad, P. Zerom, R. W. Boyd, and M. Samoc, "Stimulated Rayleigh-Bragg scattering in two-photon absorbing media," Phys. Rev. A **71**, 063810 (2005).

18. Y. Silberberg and I. Bar Joseph, "Optical instabilities in a nonlinear Kerr medium," J. Opt. Soc. Am. B **1**, 662-670 (1984).
19. Y. Silberberg and I. Bar Joseph, "Instabilities, self-oscillation, and chaos in simple nonlinear optical interaction," Phys. Rev. Lett. **48**, 1541-1543 (1982).
20. P. Yeh, "Exact solution of a nonlinear model of two-wave mixing in Kerr media," J. Opt. Soc. Am. B **3**, 747-750 (1986).
21. R. Boyd, Nonlinear Optics (Academic Press, New York, 1992).
22. G. S. He, J. Swiatkiewicz, Y. Jiang, P. N. Prasad, B. A. Reinhardt, L. –S. Tan, and R. Kannan, "Two-photon excitation and optical spatial-profile reshaping via a nonlinear absorbing medium," J. Phys. Chem. A **104**, 4805-4810 (2000).
23. J. E. Rogers, J. E. Slagle, D. G. McLean, R. L. Sutherland, B. Sankaran, R. Kannan, L. –S. Tan, and P. A. Fleitz, "Understanding the one-photon photophysical properties of a two-photon absorbing chromophore," J. Phys. Chem. A **108**, 5514-5520 (2004).
24. R. L. Sutherland, *Handbook of Nonlinear Optics*, Second Edition (Marcel Dekker, New York, 2003).
25. N. Tang and R. L. Sutherland, "Time-domain theory for pump-probe experiments with chirped pulses," J. Opt. Soc. Am. B **14**, 3412-3423 (1997).
26. A. Dogariu, T. Xia, D. J. Hagan, A. A. Said, E. W. Van Stryland, and N. Bloembergen, "Purely refractive transient energy transfer by stimulated Rayleigh-wing scattering, J. Opt. Soc. Am. B **14**, 796-803 (1997).
27. A. Dogariu and D. J. Hagan, "Low frequency Raman gain measurements using chirped pulses, Opt. Express **1**, 73-76 (1997).
28. M. Rumi and J. W. Perry, "Investigation on Air Force two-photon dyes," unpublished Air Force report, University of Arizona, Tucson, Arizona, March 2002.
29. R. L. Sutherland, M. E. Brant, D. G. McLean, J. E. Rogers, B. Sankaran, S. E. Kirkpatrick, and P. A. Fleitz, paper CFF6, CLEO/IQEC Tech. Digest, Optical Society of America, 2004.
30. G. S. He, T. –C. Lin, J. Dai, P. N. Prasad, R. Kannan, A. G. Dombroskie, R. A. Vaia, and L. –S. Tan, "Degenerate two-photon-absorption spectral studies of highly two-photon active organic chromophores," J. Chem. Phys. **120**, 5275-5284 (2004).
31. R. L. Sutherland, M. C. Brant, J. Heinrichs, J. E. Rogers, J. E. Slagle, D. G. McLean, and P. A. Fleitz, "Excited state characterization and effective three-photon absorption model of two-photon-induced excited state absorption in organic push-pull charge-transfer chromophores," J. Opt. Soc. Am. B **22**, 1939-1948 (2005).
32. A. Yariv, Quantum Electronics, Third Ed. (John Wiley & Sons, New York, 1989).